

Orthogonal Nonnegative Matrix Factorization: a Maximum-Entropy-Principle Approach^{*}

Salar Basiri^{a,*}, Mustafa Kapadia^a, Srinivasa Salapaka^a

^a*Department of Mechanical Science and Engineering, University of Illinois at Urbana-Champaign, Urbana, IL, 61801, USA*

Abstract

In this paper, we introduce a new methodology to solve the orthogonal nonnegative matrix factorization (ONMF) problem, where the objective is to approximate an input data matrix by a product of two nonnegative matrices, the features matrix and the mixing matrix, where one of them is orthogonal. We show how the ONMF can be interpreted as a specific facility-location problem (FLP), and adapt a maximum-entropy-principle based solution for FLP to the ONMF problem. The proposed approach guarantees orthogonality and sparsity of the features or the mixing matrix, while ensuring nonnegativity of both. Additionally, our methodology develops a quantitative characterization of “true” number of underlying features - a hyperparameter required for the ONMF. An evaluation of the proposed method conducted on synthetic datasets, as well as a standard genetic microarray dataset indicates significantly better sparsity, orthogonality, and performance speed compared to similar methods in the literature, with comparable or improved reconstruction errors.

Keywords: NMF, orthogonal, sparsity, microarray, pattern recognition, feature extraction

1. Introduction

In many data science applications, where large datasets contain records of many member elements, there is a need for identifying common *features* across the members and quantify the *weight* of these features in each member. In many applications, the underlying data is represented by *nonnegative real numbers*, and often for deriving semantic sense from the decomposed data, it is required that features and extents too are represented by nonnegative real numbers. These problems are modeled as nonnegative matrix factorization (NMF) problems. NMF is a low-rank approximation method that takes a

^{*}This work was supported by DOE (WPI) 10809-GR and the UIUC-ZJUI Center.

^{*}Corresponding author

Email addresses: sbasiri2@illinois.edu (Salar Basiri), kapadia5@illinois.edu (Mustafa Kapadia), salapaka2@illinois.edu (Srinivasa Salapaka)

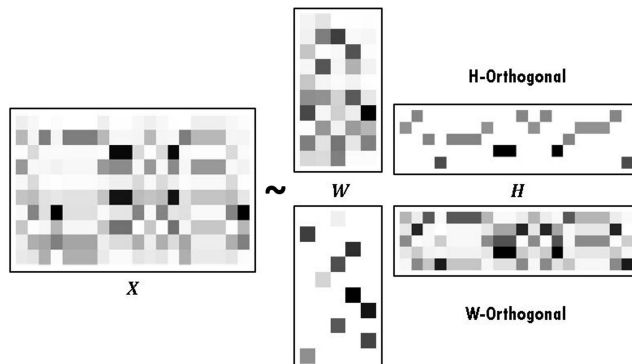


Figure 1: A visualization of the ONMF applied to the matrix X in the W -orthogonal (bottom right) and H -orthogonal case (top right).

nonnegative data matrix as input and returns a set of nonnegative features that when linearly combined together approximate the original data. More precisely, given a large data matrix $X \in \mathbb{R}_+^{d \times n}$, the goal of NMF is to approximate it by a product of low-rank, nonnegative matrices W, H where $W \in \mathbb{R}_+^{d \times k}$ is the features matrix and $H \in \mathbb{R}_+^{k \times n}$ is the mixing matrix; Here $k \leq \min(n, d)$ is the inner dimension that determines the number of features. Each column of W is a feature that has the same dimension as of the original data, and each column of H represents the weight of each feature in the corresponding data point. NMF gained global attention after Lee and Seung used it to create a part-based representation of data [1], where the nonnegativity constraint does not allow positive-negative feature cancellation and the original data can only be reconstructed via adding nonnegative parts (segment) that may or may not be overlapping. The nonnegativity constraint on W and H often leads to a more interpretable and semantic representation of the original data points, and is suitable to decompose data that are inherently nonnegative, examples include images [2, 3], audio recordings [4, 5], biomedical data [6, 7, 8], spectrometry representations [9], and other types of data [10].

The NMF problem suffers from non-uniqueness of solutions (see section 2). Thus, a variety of additional constraints have been imposed on the W and H matrix in the literature; One of which is the orthogonality constraint, that in the single-orthogonality case requires W or H to be orthogonal matrices and in the double-orthogonality case both matrices have to be orthogonal. The constraint of both matrices being orthogonal is very restrictive, and algorithms that impose this constraint typically lead to large reconstruction errors. Also since this constraint is not required in most application areas, we focus on the single-orthogonality case.

Fig. 1 visualizes the ONMF results for a given matrix in W and H -orthogonal cases. In the W -orthogonal case, the columns of W (features) are non-overlapping, and each dimension in the original data belongs to exactly one feature. In the H -orthogonal case however, the features do overlap, but their mixing in each

data point is non-overlapping, suitable for applications where each data point should be reconstructed only by a single feature.

In our approach, we re-interpret the ONMF problem as a seemingly unrelated facility location problem (FLP). FLP is an \mathcal{NP} -hard combinatorial optimization problem that aims to allocate a set of facilities to a large set of consumer nodes such that the weighted average distance between the nodes and their assigned facility is minimized. The deterministic annealing (DA) is an algorithm that successfully addresses FLPs arising in areas such as data compression and pattern recognition tasks [11]. Instead of assigning each node to one facility, the DA relaxes this hard assignment and assigns a probability distribution over all nodes that quantifies the association of each node to each facility, and employs the maximum-entropy-principle (MEP) [12] to determine the probability distribution. The DA is an iterative algorithm, where this distribution *hardens* with iterations; eventually each consumer is associated to a single facility.

Different algorithms have been developed in the literature to solve the ONMF problem. Ding et al. [13] provide an iterative update rule for ONMF, which satisfies orthogonality of features only up to a certain degree. HALS [14] proposes an improved algorithm based on ALS to satisfy the orthogonality constraint. IONMF [15] uses gradient descent to minimize the orthogonality-regularized NMF cost function based on the Frobenius norm. NLHN [16] uses a multiplicative update rule and Oja’s rule to learn nonnegative gradient projections. ONMF-A [17] uses multiplicative updates derived from the natural gradient in the Stiefel manifold to preserve the orthogonality of features. PNMF [18] solves the ONMF problem by determining a symmetric projection that maintains nonnegativity while minimizing the error. ONMF-apx [19], the most similar method to ours, views ONMF as a clustering problem and optimizes over the values of the mixing matrix to reduce the reconstruction error. ONMF-EM [20] proposes an EM-like algorithm as a solution to the weighted variant of the spherical k-means problem.

Out of the mentioned methods, only a few of them guarantee orthogonality and the ones that do usually tend to lose performance on reconstruction error, sparsity, or computational cost. They also heavily depend on the initialization of the factor matrices. In addition, these methods often assume or constrain the number of features to be known a priori. However, the resulting solution characteristics, including computation time, reconstruction errors, and the trade-off between them, depend on the choice of the number of features.

In this paper, we introduce a new algorithm, MEP-based ONMF (MEP-ONMF) that uses the DA to solve the ONMF problem. We interpret the ONMF as a facility-location problem where facilities are equivalent to the features (W) and association probabilities of the consumer nodes to facilities comprise the mixing matrix (H). We assert that using DA for solving orthogonal NMF problems provides several advantages over the state-of-the-art algorithms: (a) *invariance to initialization*: the proposed iterative algorithm evolves hierarchically, where the number of distinct features increases from one to k . Here the solution from the previous iteration serves as a *an improved guess solution* to the subsequent iteration. (b) *orthogonality and sparsity guarantee*: MEP-ONMF ensures orthogonality of the features (mixing) matrix since each row (column)

eventually has exactly one non-zero element. This also results in the maximum sparsity possible for the orthogonal factor, as no row (column) can be entirely zero when W (H) is orthogonal. (c) *detecting the true number of features*: Our approach facilitates a notion for characterizing the “true” number of underlying features. To every possible reconstruction error value, the minimum number of features that guarantees the reconstruction error is determined. The “true” number of features is defined as the number that persists for the largest range of reconstruction values. This can be very beneficial in cases such as microarray analysis as the true number of metagenes that sufficiently describe a microarray can be calculated.

Our algorithm outperforms nine other ONMF methodologies in terms of reconstruction error, sparsity, orthogonality, and computational efficiency. This has been demonstrated through simulations on synthetic matrices and a real microarray dataset, where our algorithm achieves at least the same, if not better, reconstruction error.

The paper first provides a mathematical formulation of NMF and ONMF in Section 2. Section 3 presents our proposed solution and procedure, while Section 4 outlines the experimental setup for comparing our algorithm against other methods. The experimental results and discussion are presented in Section 5, and the paper concludes with a summary and possible future directions in Sections 6 and 7.

2. Problem Formulation

Consider the data matrix $X \in \mathbb{R}_+^{d \times n}$ that we want to approximate by the product of two nonnegative matrices $W \in \mathbb{R}_+^{d \times k}$ and $H \in \mathbb{R}_+^{k \times n}$. This poses the following optimization problem:

$$\begin{aligned} \min \quad & D(X, WH) \\ \text{s.t.} \quad & W_{ij}, H_{ij} \geq 0 \quad \forall i, j \end{aligned} \tag{1}$$

where $D(X, WH)$ is the distance function between the two matrices X and WH (representing the reconstruction error), and is often chosen to be the squared Frobenius norm $\|X - WH\|_F^2$. Since there are no additional constraints on the problem, if a solution (W^*, H^*) exists, any other pair of the form $(W^*B, B^{-1}H^*)$ is also a solution to the problem, for any invertible matrix B . Therefore, the solution is not unique.

The orthogonal NMF (ONMF) requires one of the matrices W (H) to be orthogonal. Thus, the ONMF poses the following problem:

$$\begin{aligned} \min \quad & D(X, WH) \\ \text{s.t.} \quad & HH^\top = I \\ & W_{ij}, H_{ij} \geq 0 \quad \forall i, j \end{aligned} \tag{2}$$

where an additional orthogonality constraint on H has been added to the original problem. The orthogonality constraint may be replaced by $W^\top W = I$.

Note that the nonnegativity and orthogonality constraints imply that matrices can have only one non-zero element in each row (column) when W (H) is orthogonal. For instance, when W is orthogonal, since for all $i \neq j$, we have $[W^\top W]_{ij} = 0 \implies \sum_k W_{ki}W_{kj} = 0 \Rightarrow W_{ki}W_{kj} = 0$ for each k . This is possible only when at most one term in each k^{th} row is not zero. In the ONMF case, the solution pair (W^*, H^*) becomes unique, since the matrix B can only be the different permutations of rows/columns of I , the identity matrix, which is equivalent to re-numbering of the features. More specifically, any W^*B and $B^\top H^*$ where $BB^\top = I$ is also a solution to the ONMF problem as $W^*BB^\top H^* = W^*H^*$; However, If $B \neq I$ or the permutation matrix (which is simply re-ordering rows/columns of I) then the orthogonality of B mandates having at least one off-diagonal negative element in it. This negative element, when multiplied by orthogonal W^* or orthogonal H^* , produces at least one negative element in them that contradicts the nonnegativity condition. Thus, the only possible candidate for B is different permutations of the identity matrix.

3. Maximum-Entropy-Principle (MEP) Approach to Solve ONMF

3.1. ONMF as a facility-location Problem

In this paper, we interpret the ONMF as a facility-location problem. FLP is an \mathcal{NP} -hard combinatorial optimization problem that aims to allocate a set of k facilities y_j to a large set of n consumer nodes x_i such that the weighted average distance between the nodes and their assigned facility is minimized. That is,

$$\min_{y_j, \chi_{j|i}} \sum_{i,j=1}^{nk} p_i d(x_i, y_j) \chi_{j|i},$$

where $d(x_i, y_j)$ is a function of $x_i - y_j$ that represents the distance between the i^{th} node and j^{th} facility, $p_i \in [0, 1]$ is a priori known weight that gives the relative importance of the i^{th} node ($\sum_i p_i = 1$ and $p_i = 1/n$ when all the nodes are of equal importance), and the binary variable $\chi_{j|i} \in \{0, 1\}$ is 1 only when i^{th} node is assigned the j^{th} facility. If we use the notations $X = [x_1 \ x_2 \ \cdots \ x_n] \in \mathbb{R}^{d \times n}$, $Y = [y_1 \ y_2 \ \cdots \ y_k] \in \mathbb{R}^{d \times k}$, and $\chi = [\chi_{j|i}] \in \{0, 1\}^{k \times n}$, then the above optimization problem can be re-written as

$$\min_{Y, \chi} D(X, Y\chi), \text{ subject to } \chi\chi^\top = I,$$

where $D(X, Y\chi) = \sum_{i,j=1}^{kn} p_i d(x_i, y_j) \chi_{ji}$ and $I \in \mathbb{R}^{k \times k}$ identity matrix. Here $\chi\chi^\top = I$ enforces the condition that only one facility is assigned to each consumer node. This formulation is analogous to the ONMF problem formulation. Therefore, for any given nonnegative matrix $X \in \mathbb{R}_+^{d \times n}$, we can view the columns of X as the nodes locations, hence the resulting facility-location matrix $Y \in \mathbb{R}_+^{d \times k}$ and the assignment matrix $\chi \in \{0, 1\}^{k \times n}$ are both nonnegative, χ is an orthogonal matrix, and $X \approx Y\chi$. Therefore, this case is equivalent to the ONMF problem with H -orthogonal constraint, taking $W \leftarrow Y$ and $H \leftarrow \chi$. For the W -orthogonal

case, we just need to transpose the data matrix $X \leftarrow X^\top$. Following the same reasoning, $W^\top W = I$ putting $W \leftarrow \chi^\top$ and $H \leftarrow Y^\top$.

3.2. MEP-based Solution

Note that FLP (and therefore ONMF) problems are optimization problems, where a great deal of complexity arises from the constraint on decision variables $\chi_{j|i}$ to be binary variables. In the DA algorithm, these hard assignments $\chi_{j|i}$ are replaced by soft assignments $p_{j|i} \in [0, 1]$; Here the probability mass function (PMF) $p_{j|i}$ associates i^{th} data point x_i to the feature w_j . DA is an iterative algorithm where a closely related problem to (2) is addressed; this problem is given by

$$\min_{\{p_{j|i}\}, \{w_j\}} \mathcal{F} = \mathcal{D}(\{p_{j|i}\}, \{w_j\}) - \frac{1}{\beta} \mathcal{H}(\{p_{j|i}\}), \quad (3)$$

where $\mathcal{D}(\{p_{j|i}\}, \{w_j\}) = \sum_{i=1}^n p_i \sum_{j=1}^k p_{j|i} d(x_i, w_j)$ is the expected value of the cost function in (2), while the Shannon entropy $\mathcal{H}(\{p_{j|i}\}) = \sum_{i=1}^n p_i \sum_{j=1}^k p_{j|i} \log p_{j|i}$ is a measure of randomness (uncertainty) of the associated PMF $\{p_{j|i}\}$. $1/\beta$ characterizes the relative importance of the target cost function and the extent of randomness introduced in the formulation due to the PMF. Note that for a fixed β , \mathcal{F} is convex with respect to $\{p_{j|i}\}$; and as dictated by MEP, the optimal solutions for the PMF are obtained by setting $\frac{\partial \mathcal{F}}{\partial p_{j|i}} = 0$. Assuming Euclidean distance for $d(\cdot, \cdot)$, the PMF is given by

$$p_{j|i} = \frac{e^{-\beta \|x_i - w_j\|^2}}{\sum_{m=1}^k e^{-\beta \|x_i - w_m\|^2}}. \quad (4)$$

On substituting this PMF in (3), we get a revised optimization problem

$$\min_{\{w_j\}} \tilde{\mathcal{F}} = \sum_{i=1}^n p_i \log \sum_{j=1}^k e^{-\beta \|x_i - w_j\|^2}. \quad (5)$$

In this formulation, we have treated all the features (characterized by value $\{w_j\}$) to be of equal importance; a relative weight λ_j can be assigned to the j^{th} feature by assuming that λ_j units of j^{th} feature occur at value w_j ; whereby we can reinterpret distribution in (4) as

$$p_{j|i} = \frac{\lambda_j e^{-\beta \|x_i - w_j\|^2}}{\sum_{m=1}^k \lambda_m e^{-\beta \|x_i - w_m\|^2}}, \quad (6)$$

and consider a revised formulation of the problem (5)

$$\min_{\{w_j\}, \{\lambda_j\}} \bar{\mathcal{F}} = \sum_{i=1}^n p_i \log \sum_{j=1}^k \lambda_j e^{-\beta \|x_i - w_j\|^2} + \mu \left(\sum_{j=1}^k \lambda_j - 1 \right), \quad (7)$$

where the second term imposes the constraint that $\sum_{j=1}^k \lambda_j = 1$. The locally optimal values of $\{w_j\}, \{\lambda_j\}$ are determined by setting $\frac{\partial F}{\partial w_j} = 0$ and $\frac{\partial F}{\partial \lambda_j} = 0$; which yield

$$w_j = \sum_{i=1}^n p_{i|j} x_i \text{ and } \lambda_j = \sum_{i=1}^n p_i p_{j|i}, \quad (8)$$

where $p_{i|j} = p_i p_{j|i} / \lambda_j$. Thus, we get optimal (local) solutions for $\{p_{j|i}\}$ and $\{w_j\}$ at a fixed β , and we can form the matrices W and H simply by putting $W_{:j} = w_j$ and $H_{ij} = p_{j|i}$.

3.3. Phase Transitions and True Number of Features

The proposed method in section 3.2 evolves hierarchically with respect to β , as β is increased from small (≈ 0) to a high ($\approx \infty$) value; at each iteration the solutions from the previous iteration are used for initialization. Note that at initial iterations (when $\beta \approx 0$), higher emphasis is given to the randomness of associations (characterized by \mathcal{H} in (3)); hence the ensuing solutions are uniform PMF $p_{j|i} \approx \frac{1}{k} \forall i$, and all w_j are coincident the centroid of data points x_i . This is evident by looking at equations (6) and (8) at $\beta \approx 0$. Therefore all the k features are coincident at the centroid when $\beta \approx 0$. This can be also explained since the term $\sum_j e^{-\beta \|x_i - w_j\|^2}$ in $\bar{\mathcal{F}}$ cannot distinguish different summands since $\|x_i - w_j\|^2 \ll \frac{1}{\beta}$ for all j at each i . Thus $1/\beta$ acts as a resolution measure on reconstruction error (cost value in (2)); and when this resolution yardstick is too large, one feature is enough to *achieve* that resolution in reconstruction error. As β is increased, this resolution yardstick becomes smaller (finer); whereby $\|x_i - w_j\|^2$ for different j s are more *distinguishable*. As β is increased from 0, there is a critical value β_{cr} beyond which it is not possible to achieve the now smaller resolution on reconstruction error by a *single* distinct value of w_j but requires at least two distinct features. Thus as the resolution ($1/\beta$) or reconstruction error bound is decreased; more number of *distinct* features appear in the optimal solutions at successive values of β_{cr} . This *phase transition* behavior is quantified in [11].

In the context of NMF and ONMF algorithms, it is common to assume that the number of features is known a priori, or to constrain it in some way. However, we can utilize the phase transition concept to identify the true number of features present in a dataset. We adapt the notions developed in [21] in the context of the clustering problem to our problem. Based on the phase transitions at successive critical temperatures, we define a measure $\Delta(m) = \frac{\beta_{cr}(m+1)}{\beta_{cr}(m)}$ that quantifies *persistence* of m distinct features - Here $\Delta(m)$ quantifies the range of reconstruction error bounds (characterized by $1/\beta$) for which m is the smallest number of distinct features necessary (and enough) to guarantee those bounds. The true number of features is then defines as one that persists for the largest range of reconstruction errors. More precisely, *true* number m^* of features is one that satisfies $m^* = \arg \max \Delta(m)$. See Fig. 2 for a visual illustration.

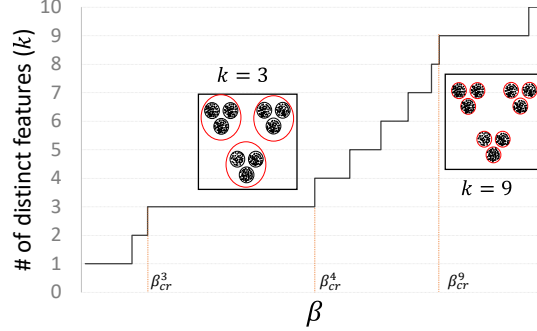


Figure 2: An instance of the phase transition phenomenon, where β_{cr} are linked with each discontinuity in the number of distinct features k . An inverse correlation between larger β values and finer resolution in decomposition is evident. The presented dataset contains either three or nine discernible features, contingent on the resolution chosen for analysis. $k = 3$ and $k = 9$ persist over a larger range of resolutions than other values of k , with $k = 3$ deeming the most persistent solution.

3.4. MEP-ONMF

The DA result in a mixing matrix H that the nonnegative numbers are always one, as each data point is assigned to exactly one feature, and the sum of association probabilities to all of the features for a given data point is equal to one. This is not necessary for the purpose of having non-overlapping features where HH^\top can equal to any diagonal matrix; Therefore, we optimize for each of these nonnegative values (θ_i)s to minimize the ONMF cost function. Let us take w_i be the facility that has a non-zero value for the i^{th} data point (it is unique since each data point is assigned to exactly one facility). Then, minimizing $E = \sum_{i=1}^n \|x_i - \theta_i w_i\|^2$ with respect to θ_i yields:

$$\theta_i = \frac{x_i^\top w_i}{\|w_i\|^2} \quad (9)$$

and we replace ones in the i^{th} columns of H with (θ_i) s. Therefore, our MEP-based algorithm for Orthogonal NMF (**MEP-ONMF**) is shown in Algorithm 1. In the step 1, $\lambda_{max} C_x$ represents the biggest eigenvalue of the covariance matrix of data points, and δ is a small perturbation ¹.

4. Simulation Setup

4.1. Metrics & Algorithms

To evaluate our algorithm and compare it with other existing algorithms, we use the following four metrics:

¹An implementation of the algorithm is available on a Github repository at :<https://github.com/salar96/MEP-Orthogonal-NMF>.

Algorithm 1 MEP-ONMF

Require: data matrix $X \in \mathbb{R}_+^{d \times n}$, number of features k_{\max} , α , β_{\max}

- 1: **Initialization** $\beta_{init} \leftarrow \frac{1}{2\lambda_{\max}C_x}$, $k \leftarrow 1$, $w_1 \leftarrow \sum_x xp(x)$, $\lambda_1 \leftarrow 1$, if W -orthogonal $X \leftarrow X^\top$
- 2: **Normalization** $x_j \leftarrow \frac{x_i}{\|x_i\|_2}$ for $i = 1 \dots n$
- 3: **loop** until $\beta = \beta_{\max}$
- 4: **repeat**
- 5: update $p_{j|i}$, w_j and λ_j by (6) and (8)
- 6: **until** convergence
- 7: $\beta \leftarrow \alpha\beta$
- 8: **if** $k < k_{\max}$ **then**
- 9: **for** all w_j **do**
- 10: check the phase transition condition
- 11: **if** satisfied for w_t **then**
- 12: add another feature $w_{k+1} = w_t + \delta$
- 13: $\lambda_{w_{k+1}} \leftarrow 0.5\lambda_{w_t}$, $\lambda_{w_t} \leftarrow 0.5\lambda_{w_t}$
- 14: do post-processing (9) on H
- 15: $W_{:j} \leftarrow w_j$ and $H_{ij} \leftarrow p_{j|i} \forall i, j$
- 16: if W -orthogonal: $W \leftarrow H^\top$, $H \leftarrow W^\top$
- 17: **return** W , H

(a) *Reconstruction error*: This metric shows how well the resulting features and mixing matrices can approximate the original data matrix; It is given by $E = \frac{\|X - WH\|_F}{\|X\|_F}$ where $\|\cdot\|_F$ denotes the Frobenius norm.

(b) *Orthogonality*: this metric shows how orthogonal the rows (columns) of a given matrix H (W) are. In other words, this metric can be used to realize how much the orthogonality constraint has been satisfied, and it is calculated as $O = 1 - \frac{\|GG^\top - GG^\top \odot I\|_F}{\|GG^\top\|_F}$ where \odot denotes the Hadamard product and I is the identity matrix.

(c) *Sparsity*: used to quantify the sparsity of a given matrix X defined as $S(\epsilon) = 1 - \frac{n(\epsilon)}{N}$ where $n(\epsilon) = |\{x \in X | x > \epsilon\}|$. Here $|\cdot|$ denotes the cardinality of the set.

(d) *Execution time*: The total time elapsed (T) in seconds to run the algorithm. All of the algorithms are executed using an Intel® Core™ i7-4790 CPU (@ 3.60 GHz) and each is run 5 times. The reported values for all the metrics are the average values over all runs.

We have chosen 9 algorithms in total to compare our algorithm with. These include ONMF-apx, HALS, IONMF, NLHN, ONMF-A, ONMF-Ding, ONMF-EM, PNMf, and the original NMF.

4.2. Datasets

The evaluation is done in two phases. In phase one, we ran the algorithms on random synthetic matrices; Specifically, the columns of the data matrix X

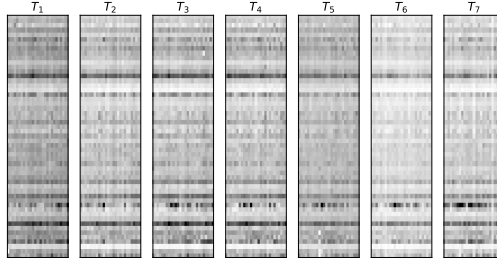


Figure 3: microarrays for different periods of time in the biological dataset [22].

were sampled from a Gamma distribution, with the probability density function defined as $P(x) = x^{\alpha-1} \frac{e^{-\frac{x}{\theta}}}{\theta^{\alpha} \Gamma(\alpha)}$ where $\Gamma(\cdot)$ is the Gamma function. Here we have chosen $\alpha = 10$ and $\theta = 1$. Additionally, a uniform random noise was incorporated into the matrix to further increase the diversity of the data. In this phase, we use $k = 20$ as the inner dimension (number of features) in all of the datasets. In phase two, we used a real-world bio-informatics dataset that contains microarrays of patients over different periods of time. Microarrays consist of nonnegative numerical data used to obtain information about gene expression patterns across different conditions. These data are usually presented in the form of gene-sample or gene-time matrices [6]. DNA microarray analysis has been widely used in many different applications, such as Tumor profiling, drug discovery, and cell behavior analysis. One important analysis conducted on these data is to decompose the microarray dataset into groups of genes that demonstrate similar expression patterns, and when combined linearly, compose the original microarray matrix [7]. This group of genes is called metagenes. For this phase, we compared our algorithm with the state of the art on the dataset provided by [22]. The dataset consists of gene expression levels for patients having multiple-sclerosis (MS) disease. The original dataset includes information on 7 time periods, 53 patients (samples) and 73 genes. However, due to missing values, we pre-processed data to get 53 genes and 27 patients over 7 time periods. Fig. 3 shows the microarrays of this dataset in the 7 different time periods. The state of the art works using this dataset have used different orthogonal NMF approaches to extract metagenes. Having the same dimension (gene number) as of the microarray, These metagenes together describe the whole microarray when linearly combined, and yet are non-overlapping, i.e. each gene only belongs to a single metagene.

5. Results and Discussion

5.1. Synthetic data

The results for synthetic matrices are reported in tables 1a-1d. In Table 1a, the underlying dataset is relatively low dimensional. Our proposed method

Table 1: Results of the simulation for 4 randomly generated datasets. E represents the reconstruction error, O . represents orthogonality, S represents sparsity and T represents performance time in seconds. d is the dimension of data points, and n is the number of data points.

| (a) $d = 10$ $n = 1000$ | | | | | (b) $d = 20$ $n = 2000$ | | | | |
|-------------------------|---------|---------|---------|---------------|---------------------------|---------|---------|---------|----------------|
| | $E(\%)$ | $O(\%)$ | $S(\%)$ | $T(s)$ | | $E(\%)$ | $O(\%)$ | $S(\%)$ | $T(s)$ |
| MEP_ONMF | 0.026 | 100 | 95 | 0.040 | MEP_ONMF | 0.027 | 100 | 95 | 0.085 |
| ONMF_apx | 0.026 | 100 | 95 | 0.133 | ONMF_apx | 0.027 | 100 | 95 | 0.264 |
| ONMF_Ding | 2.520 | 85 | 78 | 19.193 | ONMF_Ding | 0.107 | 97 | 78 | 46.584 |
| ONMF_A | 4.235 | 74 | 66 | 1.789 | ONMF_A | 4.846 | 81 | 66 | 5.930 |
| PNMF | 4.305 | 81 | 79 | 31.185 | PNMF | 4.975 | 86 | 82 | ≈ 130 |
| NHL | 5.166 | 82 | 80 | 27.051 | NHL | 6.324 | 84 | 85 | ≈ 190 |
| ONMF_EM | 9.522 | 100 | 95 | 0.086 | ONMF_EM | 8.782 | 100 | 95 | 0.201 |
| HALS | 0.006 | 13 | 24 | 2.099 | HALS | 0.483 | 13 | 29 | 2.783 |
| IONMF | 1.917 | 10 | 0 | 0.071 | IONMF | 5.006 | 11 | 0 | 0.139 |
| NMF | 0.028 | 10 | 0 | 0.348 | NMF | 0.091 | 14 | 0 | 4.788 |
| (c) $d = 50$ $n = 4000$ | | | | | (d) $d = 100$ $n = 10000$ | | | | |
| | $E(\%)$ | $O(\%)$ | $S(\%)$ | $T(s)$ | | $E(\%)$ | $O(\%)$ | $S(\%)$ | $T(s)$ |
| MEP_ONMF | 0.028 | 100 | 95 | 0.252 | MEP_ONMF | 0.028 | 100 | 95 | 0.965 |
| ONMF_apx | 0.028 | 100 | 95 | 0.420 | ONMF_apx | 0.028 | 100 | 95 | 1.239 |
| ONMF_Ding | 3.092 | 90 | 86 | ≈ 300 | ONMF_Ding | 5.375 | 87 | 87 | ≈ 1400 |
| ONMF_A | 2.130 | 90 | 61 | 17.181 | ONMF_A | 4.062 | 88 | 69 | 93.992 |
| PNMF | 7.345 | 82 | 82 | ≈ 530 | PNMF | 6.341 | 90 | 87 | ≈ 3600 |
| NHL | 6.538 | 88 | 86 | ≈ 550 | NHL | 7.718 | 86 | 89 | ≈ 3560 |
| ONMF_EM | 9.839 | 100 | 95 | 0.666 | ONMF_EM | 9.491 | 100 | 95 | 3.133 |
| HALS | 1.042 | 26 | 52 | 26.565 | HALS | 0.049 | 46 | 56 | 90.312 |
| IONMF | 7.098 | 14 | 0 | 0.314 | IONMF | 8.947 | 17 | 0 | 1.269 |
| NMF | 0.210 | 28 | 16 | 30.208 | NMF | 0.528 | 46 | 37 | ≈ 300 |

demonstrates the fastest performance time, as well as the highest levels of orthogonality and sparsity when compared to other methods. The HALS method exhibits a lower reconstruction error, but at the cost of compromised orthogonality and sparsity. Our method not only guarantees orthogonality and sparsity, but also yields a smaller reconstruction error in comparison to the original NMF method which does not have a guarantee of orthogonality or sparsity. This pattern is also observed in Tables 1b and 1c, where the dimensions of the datasets have increased significantly. In these cases, our method achieves the lowest reconstruction error among all methods. The ONMF-EM also yields orthogonality and high sparsity, however, it results in a higher reconstruction error. Finally, in Table 1d, the dataset is significantly large, and our method is demonstrated to scale well, as the performance time remains efficient in comparison to ONMF-ding, PNMf, and NHL. Our method achieves the best reconstruction error with full orthogonality, the highest sparsity, and the fastest run-time.

These results suggest that our algorithm consistently results in a sparsity of $\frac{k-1}{k}$ and guarantees orthogonality in all cases, while also scaling efficiently with the data size and yielding the lowest reconstruction error. Therefore, in scenarios where orthogonality and sparsity of the solution are important, our proposed method and ONMF-apx are the optimal choices.

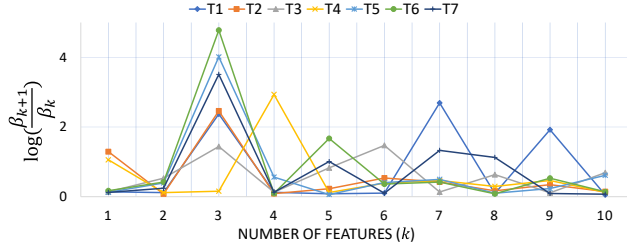


Figure 4: The logarithm of the fraction between successive critical β s over all time periods. The k^{th} value on the x-axis represents the number of features, while The y-axis shows $\log(\frac{\beta_{k+1}}{\beta_k})$ where β_k is the critical β value at which the k^{th} feature split happens.

Table 2: Simulation results for microarrays dataset

| | $E(\%)$ | $O(\%)$ | $S(\%)$ | $T(s)$ |
|-----------------|---------|---------|---------|--------|
| MEP_ONMF | 16.495 | 100 | 66 | 0.013 |
| ONMF_apx | 17.032 | 100 | 66 | 0.017 |
| ONMF_Ding | 15.704 | 94 | 33 | 0.093 |
| ONMF_A | 16.075 | 91 | 27 | 0.168 |
| PNMF | 16.601 | 90 | 34 | 0.114 |
| NHL | 16.655 | 83 | 39 | 0.134 |
| ONMF_EM | 21.444 | 100 | 66 | 0.007 |
| HALS | 15.156 | 67 | 4 | 0.156 |
| IONMF | 15.757 | 60 | 9 | 0.007 |
| NMF | 15.235 | 70 | 7 | 0.161 |

5.2. Microarrays

In this phase, we have used MEP-ONMF to extract metagenes and compare our results with other methods. The first step was to determine the number of metagenes that we want to calculate. As explained in section 3.3, the methodology of MEP-ONMF provides a feasible way to determine the true number of features in a dataset. Simply by looking at the critical β s diagram (β s at which a feature split has happened), we can determine the true number of features, and that is when a large gap is seen between two consecutive values. The logarithmic difference between successive critical β values for all time periods is depicted in Fig. 4. If a significant spike is observed at the k^{th} split, indicating a transition from k features to $k + 1$ features, it can be concluded that selecting k features yields the most persistent factorization and can thus be considered as the true number of features in the dataset. In almost all time periods, there is a large spike at the third split, except for one (T_4) where this gap happens at the fourth. Therefore, we can conclude that the true number of metagenes in this dataset is 3, which approves the number used in previous works. Tabel 2 shows the results of the simulation on the dataset, averaged over all the 7 time period and 5 runs for each algorithm in total. The results of this table indicate that our proposed algorithm is able to generate perfectly orthogonal metagenes that exhibit maximum sparsity of 67%. Additionally, the algorithm results in a smaller reconstruction error and faster performance time in comparison to other methods that do not enforce the constraint of orthogonality. It is noteworthy

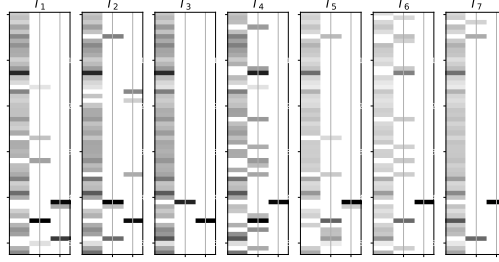


Figure 5: Orthogonal metagenes obtained via MEP-ONMF on different time periods. The y-axis corresponds to genes, while the x-axis represents each metagene.

that the IONM and HALS violate the orthogonality constraint in this case, and yield similar results to the NMF method. The closest-performing algorithm after ONMF-apx is the ONMF-EM, which has a larger reconstruction error. Therefore, for specific applications such as microarray decomposition where sparsity and orthogonality of metagenes are crucial, our proposed algorithm demonstrates better performance.

Fig. 5 gives an illustration of the metagenes calculated via MEP-ONMF for each time period. Each gene (row) belongs to exactly one *metagene* (the metagenes are non-overlapping), and therefore orthogonality of metagenes and their maximum sparsity is ensured. Some genes belong to the same *metagene* in all time periods, while the others belong to different *metagene* when time changes. The structure of metagenes is similar in different time periods, as one *metagene* contains most of the genes (has a bigger weight) and the two others contain the minority; Although small, these dissimilarities of the metagenes over different time periods might be due to experimental numerical errors related to noise and measurement error. We will discuss this more in section 7.

6. Conclusion

The paper proposes a new approach to solve the ONMF problem, which involves approximating an input data matrix using two nonnegative matrices, one of which is orthogonal. The method adapts a maximum-entropy-principle based solution for FLP to the ONMF problem and guarantees orthogonality and sparsity of the features or the mixing matrix while ensuring nonnegativity of both. The proposed method is evaluated on synthetic and genetic microarray datasets, and the results show that it outperforms similar methods in the literature in terms of sparsity, orthogonality, and performance speed with comparable or better reconstruction errors.

7. Limitation and Future works

The proposed method has limitations and potential for improvement. Fine-tuning of hyperparameters such as α and tolerance is necessary to detect the true number of features reliably. Future research could derive an explicit mathematical expression for the exact values of β at which phase transitions occur. Additionally, an extra constraint that penalizes deviation of metagenes across different time periods could be incorporated to advance the analysis of 3D microarrays.

Acknowledgment

The authors would like to thank Moses Charikar and Lunjia Hu for sharing their code in [19].

References

- [1] D. D. Lee, H. S. Seung, Learning the parts of objects by non-negative matrix factorization, *Nature* 401 (1999) 788–791. URL: <https://doi.org/10.1038/2F44565>. doi:10.1038/44565.
- [2] X. Li, L. Wang, Q. Cheng, P. Wu, W. Gan, L. Fang, Cloud removal in remote sensing images using nonnegative matrix factorization and error correction, *ISPRS Journal of Photogrammetry and Remote Sensing* 148 (2019) 103–113. URL: <https://doi.org/10.1016/2Fj.isprsjprs.2018.12.013>. doi:10.1016/j.isprsjprs.2018.12.013.
- [3] X.-R. Feng, H.-C. Li, J. Li, Q. Du, A. Plaza, W. J. Emery, Hyperspectral unmixing using sparsity-constrained deep nonnegative matrix factorization with total variation, *IEEE Transactions on Geoscience and Remote Sensing* 56 (2018) 6245–6257. doi:10.1109/TGRS.2018.2834567.
- [4] S. Makino, *Audio source separation*, volume 433, Springer, 2018.
- [5] J.-R. Gloaguen, A. Can, M. Lagrange, J.-F. Petiot, Road traffic sound level estimation from realistic urban sound mixtures by non-negative matrix factorization, *Applied Acoustics* 143 (2019) 229–238.
- [6] F. Esposito, N. D. Buono, L. Selicato, Nonnegative matrix factorization models for knowledge extraction from biomedical and other real world data, *PAMM* 20 (2021). URL: <https://doi.org/10.1002/2Fpamm.202000032>. doi:10.1002/pamm.202000032.
- [7] P. Carmona-Saez, R. D. Pascual-Marqui, F. Tirado, J. M. Carazo, A. Pascual-Montano, Biclustering of gene expression data by non-smooth non-negative matrix factorization, *BMC Bioinformatics* 7 (2006). URL: <https://doi.org/10.1186/2F1471-2105-7-78>. doi:10.1186/1471-2105-7-78.

- [8] D. Song, K. Li, Z. Hemminger, R. Wollman, J. J. Li, scPNMF: sparse gene encoding of single cells to facilitate gene selection for targeted gene profiling, *Bioinformatics* 37 (2021) i358–i366. URL: <https://doi.org/10.1093/bioinformatics/btab273>. doi:10.1093/bioinformatics/btab273.
- [9] G. F. Trindade, M.-L. Abel, J. F. Watts, Non-negative matrix factorisation of large mass spectrometry datasets, *Chemometrics and Intelligent Laboratory Systems* 163 (2017) 76–85. URL: <https://doi.org/10.1016/j.chemolab.2017.02.012>. doi:10.1016/j.chemolab.2017.02.012.
- [10] P. Weiderer, A. M. Tomáček, E. W. Lang, A nmf-based extraction of physically meaningful components from sensory data of metal casting processes, *Journal of Manufacturing Systems* 54 (2020) 62–73. URL: <https://www.sciencedirect.com/science/article/pii/S0278612519300858>. doi:<https://doi.org/10.1016/j.jmsy.2019.09.013>.
- [11] K. Rose, Deterministic annealing for clustering, compression, classification, regression, and related optimization problems, *Proceedings of the IEEE* 86 (1998) 2210–2239. doi:10.1109/5.726788.
- [12] J. Karmeshu, Entropy measures, maximum entropy principle and emerging applications, Springer Science & Business Media, 2003.
- [13] C. Ding, T. Li, W. Peng, H. Park, Orthogonal nonnegative matrix t-factorizations for clustering, in: *Proceedings of the 12th ACM SIGKDD international conference on Knowledge discovery and data mining*, 2006, pp. 126–135.
- [14] B. Li, G. Zhou, A. Cichocki, Two efficient algorithms for approximately orthogonal nonnegative matrix factorization, *IEEE Signal Processing Letters* 22 (2015) 843–846. doi:10.1109/LSP.2014.2371895.
- [15] M. Stražar, M. Žitnik, B. Zupan, J. Ule, T. Curk, Orthogonal matrix factorization enables integrative analysis of multiple RNA binding proteins, *Bioinformatics* 32 (2016) 1527–1535. URL: <https://doi.org/10.1093/bioinformatics/btw003>. doi:10.1093/bioinformatics/btw003.
- [16] Z. Yang, J. Laaksonen, Multiplicative updates for non-negative projections, *Neurocomputing* 71 (2007) 363–373. URL: <https://www.sciencedirect.com/science/article/pii/S0925231207000318>. doi:<https://doi.org/10.1016/j.neucom.2006.11.023>, dedicated Hardware Architectures for Intelligent Systems Advances on Neural Networks for Speech and Audio Processing.
- [17] S. Choi, Algorithms for orthogonal nonnegative matrix factorization, 2008 IEEE International Joint Conference on Neural Networks (IEEE World Congress on Computational Intelligence) (2008) 1828–1832.

- [18] Z. Yuan, E. Oja, Projective nonnegative matrix factorization for image compression and feature extraction, in: H. Kalviainen, J. Parkkinen, A. Kaarna (Eds.), *Image Analysis*, Springer Berlin Heidelberg, Berlin, Heidelberg, 2005, pp. 333–342.
- [19] M. Charikar, L. Hu, Approximation algorithms for orthogonal non-negative matrix factorization, 2021. URL: <https://arxiv.org/abs/2103.01398>. doi:10.48550/ARXIV.2103.01398.
- [20] F. Pompili, N. Gillis, P.-A. Absil, F. Glineur, Two algorithms for orthogonal nonnegative matrix factorization with application to clustering, *Neurocomputing* 141 (2014) 15–25. URL: <https://www.sciencedirect.com/science/article/pii/S0925231214004068>. doi:<https://doi.org/10.1016/j.neucom.2014.02.018>.
- [21] A. Srivastava, M. Baranwal, S. Salapaka, On the persistence of clustering solutions and true number of clusters in a dataset, in: *Proceedings of the AAAI Conference on Artificial Intelligence*, volume 33, 2019, pp. 5000–5007.
- [22] S. E. Baranzini, P. Mousavi, J. Rio, S. J. Caillier, A. Stillman, P. Viloslada, M. M. Wyatt, M. Comabella, L. D. Greller, R. Somogyi, X. Montalban, J. R. Oksenberg, Transcription-based prediction of response to IFN β using supervised computational methods, *PLoS Biology* 3 (2004) e2. URL: <https://doi.org/10.1371/journal.pbio.0030002>. doi:10.1371/journal.pbio.0030002.